Proceedings of ERAD 2006

Simulations of the effect of small-scale heterogeneity in rain on high-resolution research radar signals

H. Leijnse[1] **and R. Uijlenhoet**[1]

[1]Hydrology and Quantitative Water Management, Wageningen University, The Netherlands

1 Introduction

The central assumption in traditional weather radar theory is that the rain in the radar measurement volume is homogeneous (e.g. Marshall and Hitschfeld, 1953; Wallace, 1953). As can be observed in especially thunderstorms, this is far from true. In the recent literature, the discussion about how this heterogeneity can best be described (e.g. Lovejoy and Schertzer, 1990, 1995; Uijlenhoet et al., 1999; Jameson and Kostinski, 2000; Larsen et al., 2005) has not yielded a clear answer. The drop-by-drop radar signal simulator presented in this paper is a tool that can be used to test the proposed descriptions of the heterogeneity of rain. The radar signals that are generated by the simulator can be compared to actual radar measurements of rain. The discrete nature of the rain that is used in the simulator (drop-by-drop) is only necessary if the radar volume is so small that the continuity assumption of rain is no longer valid (Uijlenhoet and Sempere Torres, 2006). The Transportable Atmospheric RAdar (TARA, Heijnen et al., 2002) is an FM-CW Doppler-polarimetric research radar with a beamwidth of 2° (between the two -3 dB points) and a maximum range resolution of 2.885 m. For volumes of this size, the discrete nature of rain may become important.

The simulator is based on a marked point process such as suggested by Smith (1993). In addition to the parameters of the drop size distribution (DSD), the distribution of the raindrops in space can be supplied to the simulator. The radar volume shape and weighting functions can be defined by the user, as these may play an important role in the characteristics of the radar signal. An analysis of the sensitivity of the radar signal to the shape of the measurement volume and the weighting function may be done to determine the level of complexity that is needed in such a simulator.

Correspondence to: Hidde Leijnse
(Hidde.Leijnse@wur.nl)

The simulator will be described in Sec. 2, along with the different measurement volume shapes and weighting functions. In Sec. 3 simulations will be described. Simulations are carried out with purely homogeneous rain and with time-varying DSD parameters. These parameters are the result of the fit of gamma DSDs to a time series of measured DSDs. Conclusions will be drawn in Sec. 4.

2 Description of the simulator

Drops are generated as they arrive at a plane at the center of the radar measurement volume. Figure 1 shows the measurement volume of a radar and a possible simplification. The true radar volume is a section of a sphere, with coordinates r and θ. The cylinder that is also shown in Fig. 1 is a simplification of the measurement volume, and has the coordinates z and ρ. The third coordinate, which is the angle from the ρ (or ρ') axis perpendicular to the z (or r) axis, is not used in this paper because of symmetry.

Raindrops will be generated in the $z-\rho$ coordinate system, as they fall in the negative z direction. In the remainder of this paper, only the coordinates z and ρ for the cylindrical measurement volume will be used. However, in the case of the sperical measurement volume, these may be substituted by r and θ, respectively. In this case the coordinates of the raindrops can be transformed by

$$r = \sqrt{(z + r_0)^2 + \rho^2} \tag{1}$$

$$\theta = \arctan\left(\frac{\rho}{z+r_0}\right), \tag{2}$$

where r_0 is the range of the center of the measurement volume.

Generation of rain is done in two steps. First, a 'core' of rain is generated, which can be used in the simulation using a uniform radar volume. Secondly, 'side' rain is generated, which has properties that cause only large drops to be present away from the measurement volume center. This is done to

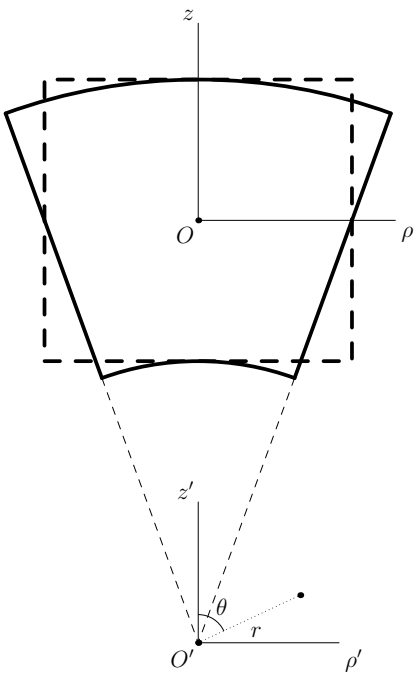

Fig. 1. The radar volume represented by either a cylinder or a section of a sphere.

save computation time and can be justified by the fact that the smaller drops have negligible contributions to the signal because of the decaying weighting function.

Positions, sizes and arrival times are generated numerically. This is done by drawing a number from a uniform distribution between 0 and 1, and setting the appropriate cumulative density function (CDF) equal to this number. The variable under consideration can then be solved from the relation thus obtained. Hence, in the remainder of this paper, CDFs of variables that are to be generated will be given.

2.1 Drop sizes

Given the number concentration in a volume of air $N_V(D)$ (mm^{-1} m^{-3}) or the number concentration in a horizontal plane per unit time $N_A(D)$ (mm^{-1} m^{-2} s^{-1}), the number concentration of drops that fall through an area A (which may be a function of the drop diameter, as will be shown later) in a time interval δt as a function of the drops diameter D is given by

$$N(D) = A\delta t \cdot v(D) \cdot N_V(D) = A\delta t \cdot N_A(D), \tag{3}$$

where $v(D)$ is the fall velocity of a drop with diameter D. The relation between v and D that will be used in this paper is the one proposed by Beard (1976). The corresponding probability density function of drop diameters is given by

$$f_D(D) = \frac{N(D)}{\int_0^\infty N(D)\mathrm{d}D}. \tag{4}$$

Drawing from this distribution involves knowledge about the cumulative distribution function, which is given by

$$F_D(D) = \int_0^D f_D(D')\mathrm{d}D'. \tag{5}$$

If we then define the following variable

$$X(D) = \int_0^D \frac{N(D')}{\delta t}\mathrm{d}D', \tag{6}$$

this cumulative distribution function can be written as

$$F_D(D) = \frac{X(D)}{X(\infty)}. \tag{7}$$

The variable $X(D)$ is introduced here because it is numerically efficient if it is used to construct a lookup table, which can also be used for the arrival process.

2.2 Drop positions

The positions of the drops projected on a plane perpendicular to the measurement volume axis is assumed to be uniformly distributed on a circle with radius ρ_0. This leads to a distribution of radial positions ρ

$$f_\rho(\rho) = \begin{cases} \frac{2}{\rho_0^2}\rho & \text{if} \quad 0 \le \rho < \rho_0 \\ 0 & \text{if} \quad \rho < 0 \bigvee \rho \ge \rho_0 \end{cases}, \tag{8}$$

with a corresponding CDF

$$F_\rho(\rho) = \left(\frac{\rho}{\rho_0}\right)^2 \qquad (0 \le \rho < \rho_0). \tag{9}$$

2.3 Drop arrival times

The drops are assumed to arrive at the plane at the center of the measurement volume according to a non-homogeneous Poisson process. In such a process, the probability of n events in a time interval τ is the following

$$p(n) = \frac{1}{n!}\left(m(t,\tau)\right)^n \mathrm{e}^{-m(t,\tau)} \tag{10}$$

where $m(t,\tau)$ is a time-integrated mean inter-arrival time

$$m(t,\tau) = \int_t^{t+\tau} \mu_n(t')\mathrm{d}t', \tag{11}$$

in which $\mu_n(t)$ ($= X(\infty)$) is the expected number of events in an area A per unit time at time t. Inter-arrival times can be drawn using the complement of the probability of zero events ($p(0)$), which is the CDF of these inter-arrival times

$$F_\tau(\tau|t) = 1 - \mathrm{e}^{-m(t,\tau)}. \tag{12}$$

2.4 Core and side rain

Raindrops are first generated for a volume that has a height h_0 and a width $2\rho_0$ ($2\theta_0$ for the spherical volume) for the entire simulation time. After this, side rain is generated based on the magnitude of the individual contributions of the raindrops. It is assumed here that the amplitude of the contribution of a drop to the total signal is given by

$$E_k = D_k^3 W_\rho(\rho_k) W_z(z_k), \tag{13}$$

where $W_\rho(\rho)$ is the measurement volume weighting function in the radial direction, $W_z(z)$ is the measurement volume weighting function in the axial direction, $\rho_k (\geq 0)$ is the radial position of the k^{th} drop and z_k is its axial position. The total signal amplitude is assumed to be approximately equal to $\sqrt{ZV}$ (Z is the reflectivity and V is the measurement volume, which is approximately given by $V = \pi \rho_0^2 h_0$). A drop will only contribute to the total radar signal if the amplitude caused by it meets the following condition

$$E_k \geq \sqrt{V \epsilon_Z}, \tag{14}$$

where ϵ_Z is the maximum allowable absolute error in Z caused by omitting a drop. Because each drop that is simulated will pass through the maximum of $W_z(z)$, this function will be set to its maximum value, which occurs at $z = 0$. Assuming $W_\rho(\rho)$ to be a monotonically decreasing function of ρ, the maximum radial distance $\rho_{max}(D)$ of a drop with diameter D can now be computed from

$$W_\rho(\rho_{max}(D)) = \frac{\rho_0 \sqrt{\pi h_0 \epsilon_Z}}{D^3 W_z(0)}. \tag{15}$$

This resulting $\rho_{max}(D)$ can then be used for the area $A = \pi \left(\rho_{max}(D)\right)^2$ in Eq. (3). After the drop diameter has been drawn, the radial distance can be drawn using Eq. (9), where ρ_0 is replaced by $\rho_{max}(D)$.

The minimum and maximum heights a drop needs to have in the simulations can be computed from

$$W_z(z_{max}(D)) = \frac{\rho_0 \sqrt{\pi h_0 \epsilon_Z}}{D^3 W_\rho(0)}. \tag{16}$$

However, if only the side (outside of a cylinder with radius ρ_0) part of the rain is considered, the maximum value of the horizontal weighting function is given by $W_\rho(\rho_0)$, so that $W_\rho(0)$ in Eq. (16) should be replaced by $W_\rho(\rho_0)$.

2.5 Signal computation

The radar signal is computed using the assumption of Rayleigh scattering

$$E(t) = \sum_k E_k(t) \mathrm{e}^{j 4\pi \frac{z_k(t)}{\lambda}}, \tag{17}$$

where λ is the radar wavelength.

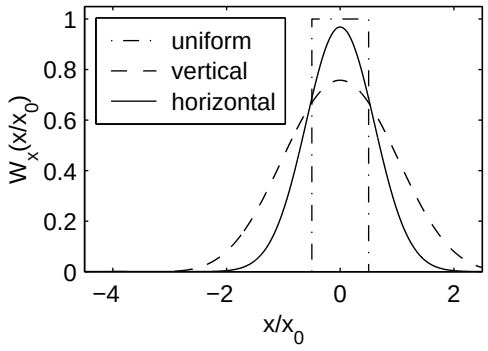

Fig. 2. Radar volume weighting functions in the horizontal (Gaussian) and vertical (Chebyshev window), with the uniform weigting function as a reference.

3 Simulation results

The simulation results presented in this paper are all with homogeneously distributed drop positions in the plane.

3.1 Drop size distributions

The drop size distributions used in the present analyses are truncated gamma distributions in either the plane (or volume, can be chosen by the user)

$$N_A(D) = \begin{cases} N_0 D^\mu \mathrm{e}^{-\Lambda D} & \text{if} \quad D_0 \leq D \leq D_1 \\ 0 & \text{if} \quad D < D_0 \bigvee D > D_1. \end{cases} \tag{18}$$

The parameters of the DSD N_0, Λ and μ can be functions of time. Two types of simulations have been carried out, one with time-varying DSD parameters, and another with constant DSD parameters. The time-varying DSD parameters are derived from measurements with an optical spectropluviometer (OSP) made in Cabauw, The Netherlands for an event with intensities exceeding 35 mm h^{-1}. The constant DSD parameters are Marshall and Palmer (1948) parameters (in the volume) for a rainfall intensity that is equal to the average of that resulting from the time-varying DSD: $N_0 = 8000\ \mathrm{mm}^{-1}\ \mathrm{m}^{-3}$, $\Lambda = 1.90\ \mathrm{mm}^{-1}$ and $\mu = 0$.

3.2 Weighting functions

The weighting function in the vertical depends on the type of radar, and on the signal processing that is used. We focus on the signal obtained with an FM-CW radar, which must be Fourier transformed (FT) to obtain profiles. A commonly used range-FT window for this type of radar is the Chebyshev window. The Chebyshev window involves a parameter that determines the sidelobe suppression level, but adversely affects the width of the corresponding resulting range cell. The antenna pattern in the horizontal is often approximated by a Gaussian function (e.g. Battan, 1973). Both of these

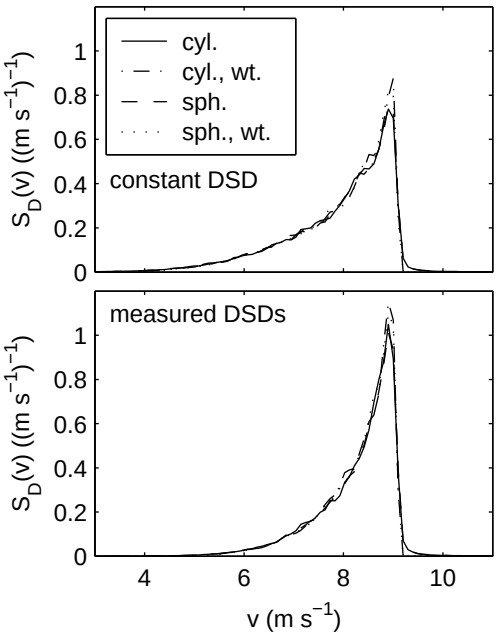

Fig. 3. Doppler spectra of the radar simulated signals for different radar volume shapes and weighting functions, for constant DSD (top) and measured (time varying) DSD (bottom).

weighting functions are shown in Fig. 2, along with the uniform weighting function as a reference.

3.3 First results

Simulations of 5 s with a sampling frequency of 1 kHz have been carried out for all measurement volume shapes and weighting functions, for rain with a constant DSD and with a time-varying DSD. The measurement volume was chosen to be at a range of 200 m, with a resolution of 3 m and a beamwidth of 2°, corresponding to the smallest TARA measurement volume. The Doppler spectra of 20 simulations have been computed over 512 samples, every 256 samples.

As a preliminary investigation of any systematic differences in the Doppler spectrum induced by differnces in measurement volume shape and weighting function, Fig. 3 shows these spectra averaged over time and over all 20 realizations, normalized by the total power. It can be seen that for these averaged spectra, the type of measurement volume does not affect the spectra very much, although the smearing of the spectrum near 9.5 m s^{-1} in the unweighted spectra due to the sharp transition in weight assigned to the drops (from 0 to 1 and vice versa) is evident. The difference in spectrum shape between the constant and measured DSDs is mainly caused by the fact that the latter has an underlying gamma DSD, whereas the former is exponential. Variations of Doppler spectra with time and between different realizations are the subject of analyses that are presently being conducted.

4 Conclusions

A radar signal simulator has been developed based on a marked point process. It has the capability to simulate radar signals with varying degrees of complexity in different measurement volume types. Time-varying DSD parameters can be supplied to the simulator, yielding the opportunity to investigate the effect of the non-homogeneity of the arrival process. The simulator will be extended in the near future to include spatial heterogeneity in the DSD as well.

Acknowledgements. Both authors are financially supported by the Netherlands Organization for Scientific Research (NWO) through a grant (nr. 016.021.003) in the framework of the Innovational Research Incentives Scheme (Vernieuwingsimpuls).

References

Battan, L. J.: Radar Observation of the Atmosphere, University of Chicago Press, 324 pp., 1973.

Beard, K. V.: Terminal velocity and shape of cloud and precipitation drops aloft, J. Atmos. Sci., 33, 851–864, 1976.

Heijnen, S. H., Ligthart, L. P., Russchenberg, H. W. J., and van der Zwan, W. F.: A high-resolution multi parameter S-band atmospheric profiler: system description and measurements, in: Proceedings of the URSI Commission F Conference 2002, Garmisch-Partenkirchen, Germany, 2002.

Jameson, A. R. and Kostinski, A. B.: Fluctuation properties of precipitation. Part VI: Observations of hyperfine clustering and drop size distribution structures in three-dimensional rain, J. Atmos. Sci., 57, 373–388, 2000.

Larsen, M. L., Kostinski, A. B., and Tokay, A.: Observations and analysis of uncorrelated rain, J. Atmos. Sci., 62, 4071–4083, 2005.

Lovejoy, S. and Schertzer, D.: Fractals, raindrops and resolution dependence of rain measurements, J. Appl. Meteorol., 29, 1167–1170, 1990.

Lovejoy, S. and Schertzer, D.: Multifractals and rain, in: New Uncertainty Concepts in Hydrology and Water Resources, edited by Kundzewicz, A. W., pp. 61–103, Cambridge University Press, 1995.

Marshall, J. S. and Hitschfeld, W.: Interpretation of the fluctuating echo from randomly distributed scatterers. Part I, Can. J. Phys., 31, 962–994, 1953.

Marshall, J. S. and Palmer, W. M.: The distribution of raindrops with size, J. Meteorol., 5, 165–166, 1948.

Smith, J. A.: Marked point process models of raindrop-size distributions, J. Appl. Meteorol., 32, 284–296, 1993.

Uijlenhoet, R. and Sempere Torres, D.: Measurement and parameterization of rainfall microstructure, J. Hydrol., in press, 2006.

Uijlenhoet, R., Stricker, J. N. M., Torfs, P. J. J. F., and Creutin, J. D.: Towards a stochastic model of rainfall for radar hydrology: Testing the Poisson homogeneity hypothesis, Phys. Chem. Earth, 24, 747–755, 1999.

Wallace, P. R.: Interpretation of the fluctuating echo from randomly distributed scatterers. Part II, Can. J. Phys., 31, 995–1009, 1953.